

Photon-energy-sensitive Si $L_{2,3}VV$ Auger satellite

J. C. Woicik and P. Pianetta

*Stanford Synchrotron and Radiation Laboratory, Stanford Linear Accelerator Center,
Stanford University, P.O. Box 4349, Stanford, California 94305*

S. L. Sorensen and B. Crasemann

Department of Physics and Chemical Physics Institute, University of Oregon, Eugene, Oregon 97403-1274

(Received 29 September 1988)

The high-energy satellite structure which appears at 103 eV kinetic energy in the Si $L_{2,3}VV$ Auger spectrum has been studied with synchrotron radiation. We find the intensity of the satellite to be sensitive to the photon energy in the vicinity of the Si K edge ($h\nu=1840$ eV). The results of an atomic Hartree-Fock Δ SCF (self-consistent field) calculation are presented which account for the energy position of the satellite, and an atomic model is described which accounts for its dependence on the excitation photon energy.

The interpretation of the Si $L_{2,3}VV$ Auger spectrum has received much theoretical and experimental attention. By dividing the valence charge into atomic and overlap components while taking into account matrix-element effects in an independent-hole one-electron formalism, Jennison¹ was able to account successfully for the experimental line shape associated with the Si $L_{2,3}VV$ Auger transition within the region of twice the valence-band width. Features lying outside of this region are assumed to be of many-body origin. More specifically, the feature which appears 17 eV below the main Auger peak has been attributed to a bulk-plasmon loss by Mularie and Rusch² while the feature which appears 15 eV above the main Auger peak has been attributed to a doubly ionized L -shell initial state by Rowe and Christman.³ It is this high-energy feature which is the focus of this work.

Figure 1 shows the Si $L_{2,3}VV$ Auger line shapes for a freshly cleaved Si(111) 2×1 surface taken with excitation photon energy $h\nu=1837$ eV (3 eV below the Si K edge) and photon energy $h\nu=1845$ eV (5 eV above the Si K edge). Experimental details have been given elsewhere.⁴ These spectra have not been corrected for background, but rather they have been scaled to make equal the number of counts above and below the pertinent spectral features (the spectrum taken with the lower-photon energy was multiplied by a factor of 15). The main peak at 88-eV kinetic energy has been attributed to pp final states, and the shoulder at 82 eV kinetic energy to sp final states. The contribution of ss final state was shown to be negligible.¹ The broad structure at 70-eV kinetic energy is the bulk-plasmon loss,² and the weak structure at 103-eV kinetic energy is the satellite Auger peak.³

In considering the nature of this high-energy feature from a simplified qualitative point of view, it is useful to note that an LVV decay will follow a KLL decay since a KLL transition leaves two $2p$ core holes in the L shell. For photon energies above the Si K edge, the $2p$ photoionization cross section is significantly smaller than the $1s$ photoionization cross section, thus the majority of L -shell

core holes will be created as a consequence of KLL decay. For photon energies below the Si K edge, there will be no KLL decays and all LVV electrons will be a consequence of direct $2p$ photoionization. The difference between the two processes, photoionization of a $2p$ electron resulting in an LVV decay versus photoionization of a $1s$ electron resulting in a KLL decay which then is followed by an LVV decay, is the presence of an additional $2p$ core hole during the LVV decay in the latter case. The final state described in the former case consists of two valence core

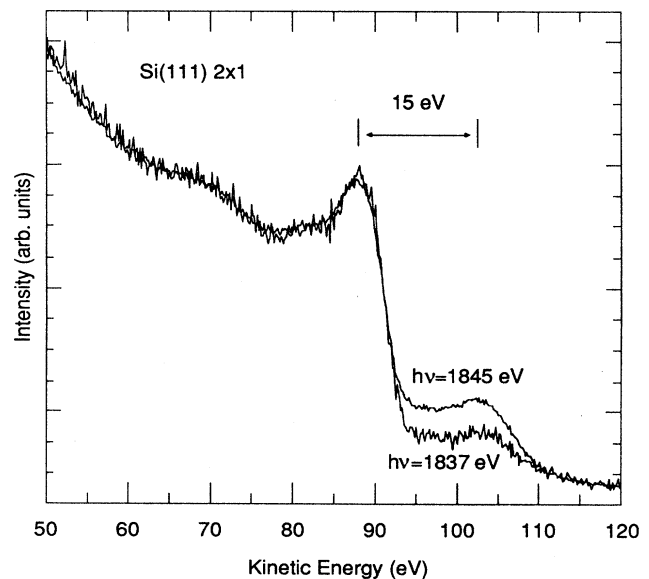


FIG. 1. The Si $L_{2,3}VV$ Auger line shape for the Si(111) 2×1 surface taken with excitation photon energy $h\nu=1837$ (3 eV below the Si K edge) and $h\nu=1845$ eV (5 eV above the Si K edge). The spectra were not corrected for background, but rather they have been scaled to make equal the intensity above and below the main spectral features.

holes and an LVV electron, while in the latter case it consists of a $2p$ core hole, two valence core holes, and an LVV electron.

These two processes are illustrated in Fig. 2; they appear to account for the satellite's photon-energy dependence. The doubly ionized L shell and the corresponding electron which contributes to the satellite Auger peak are denoted by an asterisk. The measured energy difference between the main peak, 88-eV kinetic energy, and the satellite peak, 103-eV kinetic energy, is 15 eV. Auger satellites caused by spectator holes normally are found on the low-energy side of the diagram line. The opposite situation occurring in the present case is explained by the fact that the $2p$ spectator hole lowers the $2p$ level much more than the final-state level is shifted. The observed 15-eV separation is approximately the difference between the former and twice the latter shifts.⁵ This model is consistent with the Auger spectrum observed by Rowe and Christman,³ who suggested that the satellite which they observed is due to a doubly ionized L -shell initial state produced by an incident-electron beam. The high-energy structure evident in the present data is argued here to be due to the same two-hole initial state for the LVV decay. This feature is enhanced at higher excitation energies as a consequence of prior KLL decays which arise from direct $1s$ photoionization.

In order to account for the energy positions of the Auger peaks of Fig. 1, we performed an atomic Hartree-Fock Δ SCF (self-consistent field) calculation for the atomic eigenstates associated with the electronic configurations involved in the Auger transition. In Table I we list the electronic configurations and their calculated binding energies. The listed states correspond to a vacancy in the designated orbital and have been referenced to the total energy of the neutral Si atom. Details of the calculational method that we followed and the computer code have been described by Froese-Fischer.⁶ In all cases, spin-orbit, configuration-interaction, and relativistic effects have been neglected. We have also neglected the change in atomic binding energies in going from the vapor to the solid phase since these effects can be as-

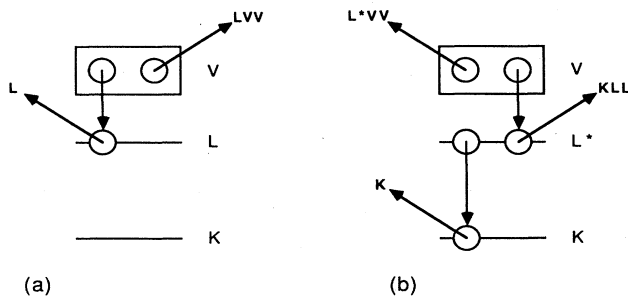


FIG. 2. Diagrams for the Si $L_{2,3}VV$ Auger decay. (a) The standard LVV decay which follows $2p$ photoionization. (b) The satellite LVV decay which follows KLL decay. The doubly ionized L shell and corresponding satellite LVV electron are marked with an asterisk.

TABLE I. The Hartree-Fock Δ SCF eigenvalues for the electronic configurations involved in the Auger transitions of Fig. 2.

State	Binding energy (eV)
$ -\rangle$	0.00
$ 2p\rangle$	108.17
$ 2p2p\rangle$	248.53
$ 3s3s\rangle$	38.42
$ 3s3p\rangle$	30.65
$ 3p3p\rangle$	22.82
$ 2p3s3s\rangle$	173.25
$ 2p3s3p\rangle$	162.88
$ 2p3p3p\rangle$	155.05

sumed to be small within the framework of our approximation. What is clear from the calculation is that the energy difference between a $2p$ core hole in a singly ionized L shell versus a $2p$ core hole in a doubly ionized L shell is 16 eV. This result is derived by taking the difference between the binding energy of the state $|2p\rangle$ and one-half of the binding energy of the state $|2p2p\rangle$. Thus, we see that the contribution of the extra "spectator" hole does indeed lower the binding energy of the $2p$ core level by slightly more than the observed separation of the high-energy satellite from the diagram Auger line.

In Table II we list the Auger transitions schematically depicted in Fig. 2, along with their respective transition energies for the atomic and the solid states. The transition energies for the atomic state are simply the difference between the initial- and final-state energies. The transition energies for the solid state have been adjusted by the addition of the "solid-state correction term" determined by Larkins⁷ and also for the Si work function.⁸ The solid-state correction arises from the increased screening of holes by the valence electrons in the solid. The magnitude of this effect has been calculated by Larkins⁷ from Slater integrals and a screening parameter; it is assumed to be the same for all Auger transitions. Since this energy corresponds to the screening of two final-state holes, for the satellite Auger transition we have incorporated an additional factor of one-half of its value in the calculation.

The relative contributions from the various transitions to the intensity of the main line may be estimated from the following argument. For the solid state, silicon hybridizes to a tetrahedral structure forming sp^3 hybrids, thus in going from the ground-state atomic configuration to

TABLE II. The transition energies corresponding to the Auger transitions of Fig. 2. The solid-state energies have been corrected for valence-band screening and work function.

Transition	Atomic (eV)	Solid (eV)
$ 2p\rangle \rightarrow 3s3s\rangle$	69.75	73.51
$ 2p\rangle \rightarrow 3s3p\rangle$	77.52	81.28
$ 2p\rangle \rightarrow 3p3p\rangle$	85.35	89.11
$ 2p2p\rangle \rightarrow 2p3s3s\rangle$	75.28	83.34
$ 2p2p\rangle \rightarrow 2p3s3p\rangle$	85.65	93.71
$ 2p2p\rangle \rightarrow 2p3p3p\rangle$	93.48	101.54

the ground-state solid configuration, we have $[\text{Ne}]3s^23p^2 \rightarrow [\text{Ne}]3s^13p^3$. Assuming constant values of the transition matrix elements, this hybridization scheme yields the following relative Auger intensities for the Auger final states: $|3s3s\rangle = \frac{1}{16}$, $|3s3p\rangle = \frac{6}{16}$, and $|3p3p\rangle = \frac{9}{16}$. Considering the transition energies from Table II, we can thus attribute the primary peak at 88 eV to pp final states and the shoulder at 82 eV to sp final states. The ss final states would occur at 75 eV and make a negligible contribution. Our simple model yields energies and peak intensities in excellent agreement with experiment and also with the line-shape calculations of Jennison.¹ For the satellite decay in the presence of the extra $2p$ spectator core hole, our calculation also agrees very well with the energy of the pp final-state contribution to the satellite peak. Our relative intensity arguments extend to the satellite decay.

The feature at 103 eV is the only structure in the Auger spectrum which is sensitive to the excitation photon energy. It may seem surprising that the satellite structure at 103 eV is visible in both spectra. The L_{VV} satellite in the spectrum taken with photon energy $h\nu = 1837$ eV may be attributed to multiple ionization during $2s$ photoionization. Multiple excitation processes occur frequently with atomic inner-shell photoionization.⁹ The "shakeoff" is a consequence of electron-electron correlations when atomic electron orbitals relax into a new ionic state accompanied by ejection of a second electron. In the limit of high-photon energies attained here, shake probabilities can be calculated using the sudden approximation of the perturbation theory.¹⁰ The results of our calculations performed after Ref. 10 are listed in Table III. The calculated values account for the residual intensity of the satellite line for photon energy below the Si K edge. Only shakeoff probabilities are indicated; shakeup probabilities are calculated to be ten times smaller and hence can be neglected.

The genealogical decay scheme of L vacancies is necessary for a quantitative consideration of the satellite-to-main-line intensity. Since the difference in their binding energies is only 0.6 eV, no distinction will be made between the L_2 and L_3 subshells. For photon energies below the Si K edge, when only L electrons are ionized, the $L_1:L_{2,3}$ -vacancy distribution is 14:10 if it is the same for Si as for Ar (Ref. 11). Nearly all L_1 vacancies decay via Coster-Kronig transitions to an $L_{2,3}$ vacancy state. These low-energy transitions are very fast, occurring before the L_{VV} decay takes place. The $L_{2,3}$ vacancies will decay via L_{VV} Auger transitions further augmenting the intensity of the diagram line.

For photon energies above the Si K edge, the situation is markedly different. The $1s$ photoionization cross section is 15 times larger than the combined $2s$ and $2p$ cross sections.¹² KLL Auger transitions dominate the decay

TABLE III. The relative shakeoff probabilities during photoionization of the $2s$ and $2p$ core levels in the high photon-energy limit.

Shakeoff probabilities during photoionization		
	2s photoionization	
2p shakeoff		8.7%
2s shakeoff		0.1%
	2p photoionization	
2p shakeoff		1.7%

scheme although 5% of the K vacancies are filled by an L electron accompanied by x-ray emission,¹³ and 12% decay through KLV transitions.¹¹ The L_1 vacancies produced during KLL Auger decay will bubble up to the $L_{2,3}$ shell via Coster-Kronig transitions. The net result of the K ionization will thus be an increase in the number of $L_{2,3}$ vacancies in the atom. Single $L_{2,3}$ -hole states will increase by a factor of 5 due to K x-ray and KLV decays. The states produced by KLL transitions will subsequently decay in the presence of an $L_{2,3}$ spectator, increasing the intensity of the satellite line by a factor of 10 in the unscaled data. The main line will then be enhanced by the L_{VV} decay of the second $L_{2,3}$ vacancy. Direct $2s$ and $2p$ photoionization contributes 7% to the main line. The above genealogy accounts for the observed 4:10 satellite to main-line intensity ratio in spectra excited with photon energies above the Si K edge. The width of the satellite peak is broader than the main line due to the shorter lifetime of the doubly ionized state.

In summary, we have studied the photon-energy dependence of the Si $L_{2,3}VV$ Auger satellite. The intensity of the satellite relative to the main line was found to increase when excited with photons of energy above the Si K edge compared with spectra excited by photons with energy below the Si K edge. Atomic calculations account for the Auger energies of both the satellite and main lines, while an atomic decay scheme accounts for the satellite's photon-energy dependence. The intensity of the satellite peak for photon energy below the Si K edge can be attributed to shake processes.

The authors acknowledge the help of B. B. Pate throughout the course of this experiment. This work was performed at the Stanford Synchrotron Radiation Laboratory, which is supported by U.S. Department of Energy under Contract No. DE-AC03-82ER13000, Office of Basic Energy Sciences, Division of Chemical/Material Sciences, and at the University of Oregon by National Science Foundation (NSF) Grant No. PHY-85-16788 and by U.S. Air Force Office of Scientific Research Grant No. AFOSR-87-0026.

¹D. R. Jennison, Phys. Rev. Lett. **40**, 807 (1978).

²W. M. Mularie and T. W. Rusch, Surf. Sci. **19**, 469 (1970).

³J. E. Rowe and S. B. Christman, Solid State Commun. **13**, 315 (1973).

⁴J.C. Woicik, B. B. Pate, and P. Pianetta, Phys. Rev. B (to be published).

⁵D. Burch, L. Wilits, and W. E. Meyerhof, Phys. Rev. A **9**, 1007 (1974).

- ⁶C. Froese-Fischer, *Comput. Phys. Commun.* **14**, 145 (1978).
⁷F. P. Larkins, *At. Data Nucl. Data Tables* **20**, 311 (1977).
⁸S. M. Sze, *Physics of Semiconductor Devices* (Wiley, New York, 1981).
⁹G. B. Armen, T. Åberg, K. R. Karim, J. C. Levin, B. Crasemann, G. S. Brown, M. H. Chen, and G. E. Ice, *Phys. Rev. Lett.* **54**, 182 (1985).
¹⁰G. B. Armen, thesis, University of Oregon, 1985; T. Åberg, *Ann. Acad. Sci. Fenn. A VI*, 308 (1969).
¹¹M. H. Chen, B. Crasemann, and H. Mark, *At. Data Nucl. Data Tables* **24**, 13 (1979).
¹²J. H. Scofield, Lawrence Livermore Laboratory Report No. UCRL-51326, 1973.
¹³M. O. Krause, *J. Phys. Chem. Ref. Data* **8**, 307 (1979).